

図1 がんサンプル集団における、異なる正の選択シグナルを示す遺伝子の例

各点 (○) は、集団中異なるサンプルに対する体細胞変異の遺伝子上の位置を示す。A) 偶然から期待されるより多くの変異が蓄積する。そのような遺伝子はその腫瘍集団に対し高頻度で変異する遺伝子として同定される。この方法においては、バックグラウンドの変異確率に影響を与えることがわかっている複数の因子を考慮に入れる必要がある。B) この遺伝子に観察される変異は強い機能的影響を引き起こすものに偏っており、このタイプの変異が選択されたこと、したがってドライバーであることを示唆している。機能的影響をスコア化するため使われる指標自体の能力が、このアプローチの性能を規定する。例えば、PIK3CA 残基1,047を変える変異はがん原的であることが知られているが、保存にもとづく機能的影響の指標では過小評価になる¹⁶⁾。なぜならこの残基は種にわたってかなり変化に富むからである。C) 本文で述べているように、この遺伝子で観察された変異は特定の領域にぎわめて集中している。BRAF 残基600のがん原変異のような機能獲得型変異は、この方法で高感度に検出される¹⁶⁾。一方、機能欠失を起こす切り詰め型変異は、遺伝子上で散らばってしまう。D) 本文で述べているように、このケースではタンパク質のリン酸化部位に変異が偏って発生する

がん狙われた変異は、タンパク質のある箇所を集積する。OncodriveCLUST¹⁶⁾はこの考えを取り入れ、変異の確率がタンパク質配列にわたって均質かを調べる。この方法では、サイレント変異を腫瘍変異の凝集度の基準線としている。この基準線を越えて非同義変異を集積している遺伝子が検出される。

4) その他の方法

他にも正の選択シグナルを検出する方法が開発されている。例えばActiveDriverは、リン酸化部位に偏って起こる体細胞変異をもつ遺伝子を検出し、それによってリン酸化ネットワークを乱すドライバーイベントを浮き彫りにする(図1D)¹⁷⁾。他に、遺伝子モジュールにおける変異を調べる方法もある。MEMOはパスウェイデータを使って、サンプル間で相互排他的なパターンにしたがう変異をもつ遺伝子の、連結クリークを検出する。この背後にある考え方は、すでに変異したパスウェイ上の別の遺伝子に変異が起きると、腫瘍細胞にさらなる選択上の利益を与えることなく、むしろ合成致死を引き起こしてしまうことである¹⁸⁾。他に、HotNetアルゴリズムは遺伝子相互作用マップ上で熱拡散モデルを使って、変異頻度のような指標値に富む遺伝子を連結しながら、かき集めてくる¹⁹⁾。

5) ベストな方法

いうまでもないことだが、手法の性能を規定するのは、つくり上げた統計的枠組みのなかで潜在的因子の複雑さがどれだけ考慮できているか、さらにはそこでの基準自体がどこまで適用できるか、である。例えば変異頻度にもとづく方法は、低頻度なドライバー変異を見逃す傾向がある。機能への影響を調べる方法は、機能喪失イベントにはより明確な結果を出すだろう。凝集している変異を同定する方法は、がん遺伝子を同定するにはよい。ベストな考えは、いくつかの方法を組み合わせることだろう。それによって、各方法の利点と欠点のバランスをとり、完全かつ確実なドライバー遺伝子のリストを得ることができる。われわれは最近このアイデアにもとづいて12の異なるがん腫の3,205サンプルを解析し、その結果291個の変異ドライバー候補を得た²⁰⁾。つまり、正の選択シグナルを相互補完的に調べる方法を組み合わせることで、真のがん遺伝子の抽出を改善できることを実証した。

最後になるが、がんドライバーとして同定された遺伝子に起こる変異のすべてが、腫瘍形成に関与しているわけではないことを強調しておく。確かにドライバー遺伝子は腫瘍表現型につながる潜在能力をもっており、ド

ライバー変異を蓄積しうる。しかしそれらはまた、パッシブ変異も蓄積しうる。個々の腫瘍の変異を評価するとき、このことは心に留めておくべきである。

3 発がんドライバーの完全なカタログ化に向けて

1) ドライバー変異のないサンプル

もちろんすべての腫瘍形成がドライバー遺伝子の変異で説明できるわけではないが、常識的な予想では、がんはその進行過程で獲得される変異によって引き起こされるはずである。しかし変異の少ないサンプルのなかには、ドライバー遺伝子にほとんど、あるいは、全く変異がないサンプルもある。この理由としては以下があげられる。まずは、変異性ドライバー遺伝子を、すべては検出できていないことである。次は、発がんイベントが非コード領域に起きていることである。3番目は、腫瘍形成が変異とは別のメカニズム（例えば、転座、コピー数変化、高メチル化）によって引き起こされているということである。とはいえ、他のメカニズムで腫瘍形成を促す遺伝子はたいてい点変異上のドライバーでもあろうから、多くの腫瘍サンプルの変異を分析すれば、がんドライバーの包括的なカタログは作製できるはずである。例えば、エピジェネティクスによるサイレンシングや遺伝子欠失の標的となるドライバーはまた、遺伝子切り詰め型の変異でもおそらく標的のはずである。コピー数増幅や遺伝子融合によるドライバーはまた、活性化変異を介したドライバーとして機能しているはずであろう²¹⁾。

2) 低頻度のドライバー

最近の研究において、がんゲノムアトラス (The Cancer Genome Atlas : TCGA) や国際がんゲノムコンソーシアム (The International Cancer Genome Consortium : ICGC) などが提供する大規模データセットから得られたドライバー遺伝子のカタログが報告されている^{2) 20) 22) 23)}。それらが示しているのは、高頻度で変異する遺伝子というものがほとんど存在しないということである²⁾。むしろ、頻度の分布を描いたとき低頻度側に長い尾を引く（したがって検出の信頼性もまた低い）、低リカレントなドライバーによって、がんの全体像は支配されているということである²⁾。いまだ体系的に研究されたことのないまれながんに関する

ものを除いて、比較的高頻度で変異する遺伝子は発見し尽くされたといえる²³⁾。対照的に、低リカレントなドライバーのカタログは、調べる症例の数が増えるほど、長くなっている。一方で、依然としてなぜ、ある種の遺伝子は他よりはるか頻繁にがんの標的となるのか、その理由はわかっていない。しかしこの疑問は、腫瘍の形成過程や腫瘍細胞が依存するメカニズムを深く理解するうえできわめて重要である。

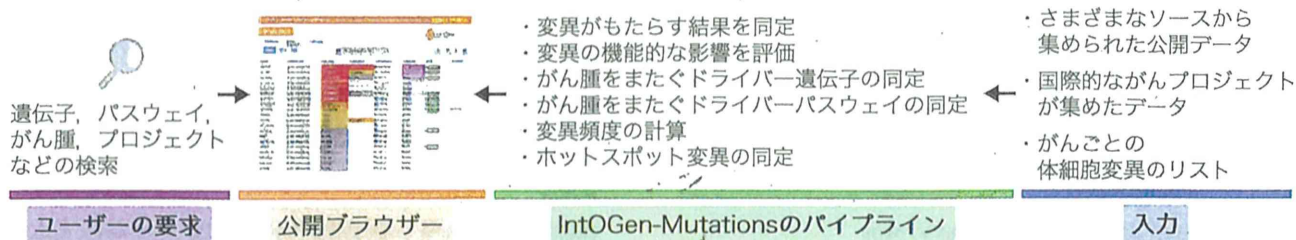
4 IntOGen-Mutations

がんゲノム研究における大きな障壁の1つは、がん再シーケンシング計画によって得られる、長大な変異のカタログを容易に分析できるバイオインフォマティクスパイプラインが不足していることである。この課題に答えるために、われわれはIntOGen-Mutations (<http://www.intogen.org/web/mutations/v04/search?1>) をつくった (図2)。これはウェブベースのツールであり、腫瘍サンプル集団のデータから発がんドライバーを同定することを目的としている。さらに、大規模な国際コンソーシアムから個々の研究室まで、それらが提供する可能な限りのがん研究データが体系的に分析されており、その結果をブラウズすることもできる。

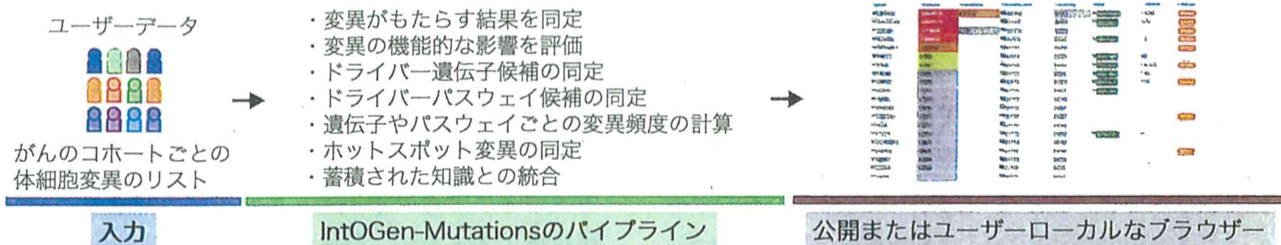
IntOGen-Mutationsの最初のリリースでは、31の異なる大規模がんプロジェクトから、4,600以上の腫瘍サンプルのデータを分析した²⁴⁾。例えば各腫瘍集団の正の選択シグナルを調べ、遺伝子・パスウェイ・組織レベルで結果を得た。加えて、興味を引く外部データベースへのリンクも提供した。

このツールは、新しいがんゲノム再シーケンシングデータを使って、定期的にアップデートされている。次のリリースでは、7,000サンプル以上の分析を網羅する予定である。すでに分析されたデータセットの結果をブラウズすることに加え、ユーザーはこのツールで自身もつ腫瘍サンプル集団や単一個体の変異を分析することもできる。分析パイプラインはわれわれのサーバー上オンラインで動かすこともできるし、ユーザーのコンピュータ上でローカルに動かすこともできる。将来のバージョンでは、治療方針決定に役立つ分子標的薬の情報も含める予定である。

A IntOGen-Mutationsでブラウザできる情報



B がんサンプル集団に対する体細胞変異の解析



C がん患者個人に対する体細胞変異の解析

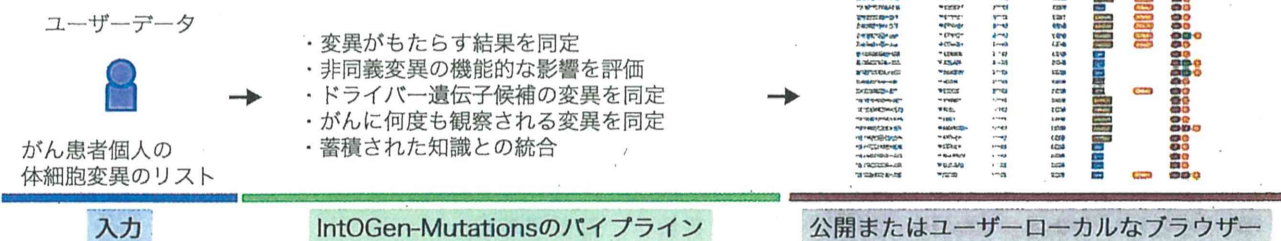


図2 IntOGen-Mutationsの使用例

A) 再シーケンシング計画によって提供される, 可能な限りのデータが体系的に分析されており, その結果をブラウザすることができる. B) 腫瘍集団における新しい体細胞変異の分析. C) 腫瘍一症例に対する体細胞変異の分析 (文献25より転載)

おわりに

がんは無数の体細胞変異がその性質を決定する不均質な病気であり, がんを理解するためにはドライバー変異をパッセンジャー変異から分離しなければならない. 次世代シーケンシング技術によって, 大規模な腫瘍集団のシーケンス分析が可能となり, それによって正の選択シグナルを介してドライバー遺伝子が検出されてきた. 各々の方法には, 結果を解釈する際注意すべき前提がある. ベストなアプローチは, 相互補完的な方法の結果を組合わせて, 各方法の利点と欠点のバランスをとることであろう²⁰⁾. この戦略を使って最

近, 既知がん遺伝子の役割が確かめられ, その知見を他の腫瘍へ拡張したり, 腫瘍進化に関連する新しい遺伝子候補や生物学的過程を発見したりすることが可能となった. この流れのなかで, 主要ながんの標的となるありふれたドライバー遺伝子の探索はほぼ終了したといえる. 一方, 頻度分布上, 長い尾を引く低頻度ドライバーは, より大規模なデータセットを分析することでさらに発見されていくであろう.

ドライバー遺伝子の包括的なカタログを作製することは, 腫瘍形成を深く理解し, 患者ごとに最適な新しい治療戦略を開発するためのさらなる解析への最初のステップとなる. ドライバーイベントが, 時間と空間

でどう作動するかを理解する必要もあるだろう。その理解のうえに、腫瘍細胞が特異的にもつ弱点を同定できれば、腫瘍細胞のクローナルな性質と、それが正常細胞と行う相互作用をも考慮した選択的治療法が設計できるようになる。究極的には実験による検証が必要であろうが、これらの結果は、分子標的薬による個別化医療の実施、免疫療法の使用、よりよい早期発見法の開発といった、より合理的で効果的ながんの病勢管理を可能とする次世代治療戦略を生み出す重要なステップとなるだろう。

(翻訳：加藤 護)

文献

- 1) Stratton MR : Science, 331 : 1553-1558, 2011
- 2) Vogelstein B, et al : Science, 339 : 1546-1558, 2013
- 3) Alexandrov LB, et al : Nature, 500 : 415-421, 2013
- 4) Stratton MR, et al : Nature, 458 : 719-724, 2009
- 5) Gonzalez-Perez A, et al : Nat Methods, 10 : 723-729, 2013
- 6) Ng PC & Henikoff S : Nucleic Acids Res, 31 : 3812-3814, 2003
- 7) Adzhubei IA, et al : Nat Methods, 7 : 248-249, 2010
- 8) Reva B, et al : Nucleic Acids Res, 39 : e118, 2011
- 9) González-Pérez A & López-Bigas N : Am J Hum Genet, 88 : 440-449, 2011
- 10) Shihab HA, et al : Bioinformatics, 29 : 1504-1510, 2013
- 11) Carter H, et al : Cancer Res, 69 : 6660-6667, 2009
- 12) Gonzalez-Perez A, et al : Genome Med, 4 : 89, 2012
- 13) Dees ND, et al : Genome Res, 22 : 1589-1598, 2012
- 14) Lawrence MS, et al : Nature, 499 : 214-218, 2013
- 15) Gonzalez-Perez A & Lopez-Bigas N : Nucleic Acids Res, 40 : e169, 2012
- 16) Tamborero D, et al : Bioinformatics, 29 : 2238-2244, 2013
- 17) Reimand J & Bader GD : Mol Syst Biol, 9 : 637, 2013
- 18) Ciriello G, et al : Genome Res, 22 : 398-406, 2012
- 19) Vandin F, et al : Genome Res, 22 : 375-385, 2012
- 20) Tamborero D, et al : Sci Rep, 3 : 2650, 2013
- 21) Tamborero D, et al : PLoS One, 8 : e55489, 2013
- 22) Kandath C, et al : Nature, 502 : 333-339, 2013
- 23) Lawrence MS, et al : Nature, 505 : 495-501, 2014
- 24) Gonzalez-Perez A, et al : Nat Methods, 10 : 1081-1082, 2013

<著者プロフィール>

Nuria Lopez-Bigas : スペイン・バルセロナのポンペウ・ファブラ大学 (Universitat Pompeu Fabra) ・生物医学ゲノムグループ (Biomedical Genomics group) リーダー。2002年、バルセロナがん研究所 (the Oncologic Research Institute) にて聴力障害の分子的基础の研究で博士号を取得。イギリスのケンブリッジの European Bioinformatics Institute に移り、コンピュータによる疾病およびがん遺伝子の研究プロジェクトに参加。'06年より、ポンペウ・ファブラ大学でグループリーダーとなり、がんのゲノミクスとバイオインフォマティクスを研究。'11年より、ICREA (Institució Catalana de Recerca i Estudis Avançats) Research Professor.

Druggable Oncogene Fusions in Invasive Mucinous Lung Adenocarcinoma

Takashi Nakaoku^{1,8}, Koji Tsuta⁴, Hitoshi Ichikawa², Kouya Shiraishi¹, Hiromi Sakamoto², Masato Enari³, Koh Furuta⁴, Yoko Shimada¹, Hideaki Ogiwara¹, Shun-ichi Watanabe⁵, Hiroshi Nokihara⁶, Kazuki Yasuda⁷, Masaki Hiramoto⁷, Takao Nanno⁷, Teruhide Ishigame⁹, Aaron J. Schetter⁹, Hirokazu Okayama⁹, Curtis C. Harris⁹, Young Hak Kim⁸, Michiaki Mishima⁸, Jun Yokota^{1,10}, Teruhiko Yoshida², and Takashi Kohno¹

Abstract

Purpose: To identify druggable oncogenic fusions in invasive mucinous adenocarcinoma (IMA) of the lung, a malignant type of lung adenocarcinoma in which *KRAS* mutations frequently occur.

Experimental Design: From an IMA cohort of 90 cases, consisting of 56 cases (62%) with *KRAS* mutations and 34 cases without (38%), we conducted whole-transcriptome sequencing of 32 IMAs, including 27 cases without *KRAS* mutations. We used the sequencing data to identify gene fusions, and then performed functional analyses of the fusion gene products.

Results: We identified oncogenic fusions that occurred mutually exclusively with *KRAS* mutations: *CD74-NRG1*, *SLC3A2-NRG1*, *EZR-ERBB4*, *TRIM24-BRAF*, and *KIAA1468-RET*. *NRG1* fusions were present in 17.6% (6/34) of *KRAS*-negative IMAs. The *CD74-NRG1* fusion activated HER2:HER3 signaling, whereas the *EZR-ERBB4* and *TRIM24-BRAF* fusions constitutively activated the ERBB4 and BRAF kinases, respectively. Signaling pathway activation and fusion-induced anchorage-independent growth/tumorigenicity of NIH3T3 cells expressing these fusions were suppressed by tyrosine kinase inhibitors approved for clinical use.

Conclusions: Oncogenic fusions act as driver mutations in IMAs without *KRAS* mutations, and thus represent promising therapeutic targets for the treatment of such IMAs. *Clin Cancer Res*; 20(12); 3087–93. ©2014 AACR.

Introduction

Oncogene fusions have recently been identified as driver mutations and (possible) therapeutic targets in lung adenocarcinoma (LADC), a major histologic type of lung cancer (1). Such fusions include *EML4-ALK*, *KIF5B-ALK*, *KIF5B*, or *CCDC6-RET*, and *CD74*, *EZR*, or *SLC3A2-*

ROS1 (2–9). These oncogene fusions occur mutually exclusively with one another, and with other targetable oncogene aberrations such as *EGFR*, *KRAS*, *BRAF*, and *HER2* mutations. Therefore, molecular targeted therapy combined with the identification of driver oncogene aberrations represents a powerful and promising approach to personalized treatment of LADC (10, 11).

Invasive mucinous adenocarcinoma (IMA) of the lung is composed predominantly of goblet cells. IMA is morphologically characterized by tall columnar cells with basal nuclei and a pale cytoplasm containing varying amounts of mucin (12, 13). IMAs, which constitute 2% to 10% of all LADCs in Japan, the United States, and European countries (14–16), are indicated as being more malignant than more common types of LADC, such as acinar or papillary adenocarcinoma. The *KRAS* mutation is the only driver aberration commonly detected in IMAs (in 50%–80% of cases). To date, no driver gene aberrations have been detected in *KRAS*-negative IMAs; these aberrations must be identified to facilitate the development of effective treatments for such cancers. Therefore, we performed whole-transcriptome sequencing (RNA sequencing) of IMAs lacking *KRAS* mutations to identify novel chimeric fusion transcripts that represent potential targets for cancer therapy.

Authors' Affiliations: Divisions of ¹Genome Biology, ²Genetics, and ³Refractory Cancer Research, National Cancer Center Research Institute, Divisions of ⁴Pathology and Clinical Laboratories, ⁵Thoracic Surgery, and ⁶Thoracic Oncology, National Cancer Center Hospital, Chuo-ku; ⁷Department of Metabolic Disorder, Diabetes Research Center, Research Institute, National Center for Global Health and Medicine, Shinjuku-ku, Tokyo; ⁸Department of Respiratory Medicine, Graduate School of Medicine, Kyoto University, Yoshida-Konoe-cho, Sakyo-ku, Kyoto, Japan; ⁹Laboratory of Human Carcinogenesis, Center for Cancer Research, National Cancer Institute, NIH, Bethesda, Maryland; and ¹⁰The Institute of Predictive and Personalized Medicine of Cancer (IMPPC), Barcelona, Spain

Note: Supplementary data for this article are available at Clinical Cancer Research Online (<http://clincancerres.aacrjournals.org>).

Corresponding Author: Takashi Kohno, Division of Genome Biology, National Cancer Center Research Institute, 5-1-1 Tsukiji, Chuo-ku, Tokyo 104-0045, Japan. Phone: 81-3-3542-2511; Fax: 81-3-3542-0807; E-mail: tkkohno@ncc.go.jp

doi: 10.1158/1078-0432.CCR-14-0107

©2014 American Association for Cancer Research.

Translational Relevance

Oncogene fusions, such as the *ALK*, *RET*, and *ROS1* fusions, have recently been revealed as therapeutic targets in lung adenocarcinoma (LADC). We identified multiple druggable oncogene fusions, including those involving the *NRG1*, *ERBB4*, and *BRAF* genes, in invasive mucinous adenocarcinoma (IMA), a malignant type of LADC. The fusions occurred mutually exclusively with *KRAS* mutations, a common driver oncogene aberration in IMA. These fusions represent potentially clinically relevant targets for treatment of IMAs that lack *KRAS* mutations.

Materials and Methods

Samples

Ninety IMAs were identified among consecutive patients with primary adenocarcinoma of the lung who were treated surgically at the National Cancer Center Hospital, Tokyo, Japan, from 1998 to 2013. Histologic diagnoses were based on the most recent World Health Organization classification and the International Association for the Study of Lung Cancer/American Thoracic Society/European Respiratory Society (IASLC/ATS/ERS) criteria for LADC (13, 17). Total RNA was extracted from grossly dissected, snap-frozen tissue samples using TRIzol (Invitrogen). The study was approved by the Institutional Review Boards of the participating institutions.

RNA sequencing

RNA sequencing libraries were prepared from 1 or 2 μ g of total RNA using the mRNA-Seq Sample Prep Kit or TruSeq RNA Sample Prep Kit (Illumina). The resultant libraries were subjected to paired-end sequencing of 50 or 75 bp reads on a Genome Analyzer IIx (GAIIx) or HiSeq 2000 (Illumina). Fusion transcripts were detected using the TopHat-Fusion algorithm (18). Experimental conditions for RNA sequencing are described in Supplementary Table S1.

Examinations of oncogenic properties of fusion products

To construct lentiviral vectors for expression of the CD74-*NRG1*, *EZR-ERBB4*, and *TRIM24-BRAF* fusion proteins, full-length cDNAs were amplified from tumor cDNA by PCR and inserted into pLenti-6/V5-DEST plasmids (Invitrogen). The integrity of each inserted cDNA was verified by Sanger sequencing. Expression of fusion products of the predicted sizes was confirmed by Western blot analysis of transiently transfected and virally infected cells (Supplementary Fig. S1A). Details of plasmid transfection, viral infection, Western blot analysis, and soft agar colony and tumorigenicity assays are described in Supplementary Materials and Methods.

Results and Discussion

We prepared an IMA cohort of 90 cases consisting of 56 (62%) cases with *KRAS* mutations and 34 (38%) cases without. The 34 *KRAS*-negative cases included two, one, and one cases with *BRAF* mutation, *EGFR* mutation, and *EML4-ALK* fusion, respectively; the remaining 30 were "pan-negative" for representative driver aberrations in LADCs. Thirty-two cases, consisting of 27 pan-negative and five *KRAS* mutation-positive cases, were subjected to RNA sequencing (Supplementary Table S1). Analysis of $>2 \times 10^7$ paired-end reads obtained by RNA sequencing and subsequent validation by Sanger sequencing of reverse transcription PCR (RT-PCR) products revealed five novel gene-fusion transcripts detected only in the pan-negative IMAs: *CD74-NRG1*, *SLC3A2-NRG1*, *EZR-ERBB4*, *TRIM24-BRAF*, and *KIAA1468-RET* (Fig. 1A and B; Table 1; details in Supplementary Materials and Methods; Supplementary Fig. S2 and Supplementary Table S2). RT-PCR screening of these fusions in the remaining 58 IMAs that had not been subjected to RNA sequencing revealed one additional pan-negative case with the *CD74-NRG1* fusion. Thus, the *CD74-NRG1* fusion, detected in five of 34 (14.7%) cases negative for *KRAS* mutations, was the most frequent fusion among *KRAS* mutation-negative IMAs. Fusions of *CD74* or *SLC3A2* with *NRG1* were present in 17.6% (6/34) of cases. The five novel fusions were mutually exclusively with one another and were not present in any of the *KRAS* mutation-positive cases (Table 2).

Four of the novel fusions, *CD74-NRG1*, *SLC3A2-NRG1*, *EZR-ERBB4*, and *TRIM24-BRAF*, involved rearrangements of genes encoding protein kinases or a ligand of a receptor protein kinase (*NRG1*/neuregulin/hereregulin) for which oncogenic rearrangements have not been previously reported in lung cancer (Supplementary Fig. S3). The remaining fusion was a novel type involving the *RET* oncogene; fusions with *RET* are observed in 1% to 2% of LADCs (4, 5, 7, 8, 11). In a screen of 315 LADCs without IMA features from Japanese patients and 144 consecutive LADCs from U.S. patients, all tumors were negative for all of the *NRG1*, *BRAF*, and *ERBB4* fusions, as well as the novel *RET* fusion. Therefore, these fusions might be driver aberrations specific to LADCs with IMA features. The four novel gene fusions were likely to have been caused by interchromosomal translocations or paracentric inversion (Table 1 and Supplementary Fig. S3). Consistently, separation of the signals generated by the probes flanking the translocation sites of *NRG1* in fusion-positive tumors was observed upon FISH analysis of *CD74-NRG1* fusion-positive tumors (Supplementary Fig. S4). We also confirmed overexpression of *NRG1*, *ERBB4*, and *BRAF* proteins in tumor cells carrying the corresponding fusions by immunohistochemical analysis, using antibodies recognizing polypeptides retained in the fusion proteins; expression of *NRG1*, *ERBB4*, and *BRAF* proteins was also observed in some fusion-negative cases (Supplementary Fig. S5). IMAs harboring gene fusions were obtained from both male and female patients, although

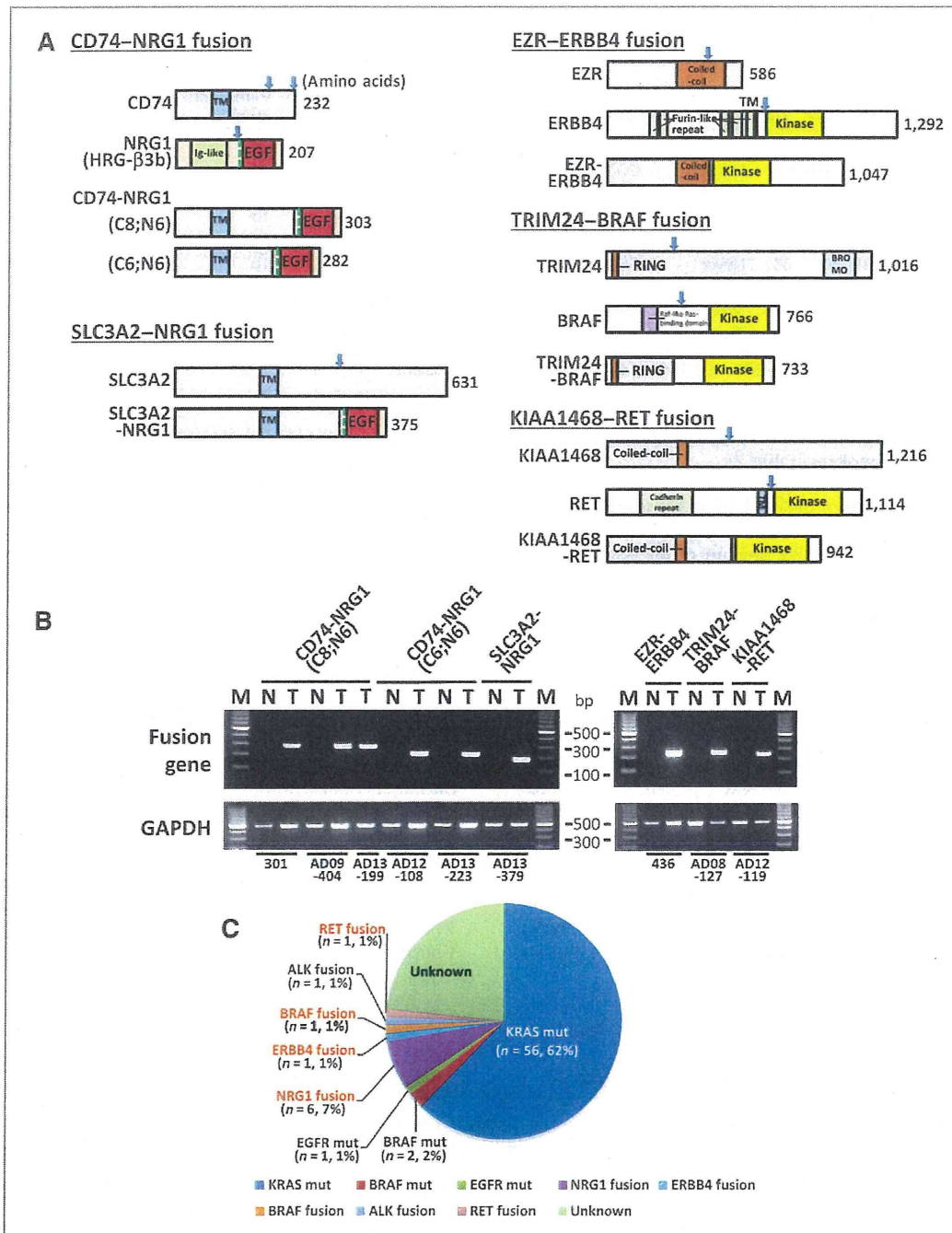


Figure 1. Oncogenic fusions in invasive mucinous LDAC. A, schematic representations of the wild-type proteins (top rows of each section) followed by the fusion proteins identified in this study. The breakpoints for each variant are indicated by blue arrows. TM, transmembrane domain. Locations of putative cleavage sites in the NRG1 polypeptide are indicated by dashed green lines. B, detection of gene-fusion transcripts by RT-PCR. RT-PCR products for glyceraldehyde-3-phosphate dehydrogenase (*GAPDH*) are shown below. Six IMAs (T) positive for gene fusions are shown alongside their corresponding non-cancerous lung tissues (N); labels below the gel image indicate sample IDs (see Table 1). C, pie chart showing the fraction of IMAs that harbor the indicated driver mutations.

Table 1. Characteristics of invasive mucinous LDACs with novel gene fusions

No.	Sample	Sex	Age	Smoking (pack/year)	Gene fusion	Chromosome aberration	Oncogene mutation ^a	Pathologic stage	TTF1	HNF4A
1	301T	M	55	Ever (47)	<i>CD74-NRG1</i>	t(5;8)(q32;p12)	None	1a	–	+
2	AD12-108T	F	68	Never	<i>CD74-NRG1</i>		None	2b	–	+
3	AD09-404T	F	78	Never	<i>CD74-NRG1</i>		None	1a	–	+
4	AD13-199T	F	47	Never	<i>CD74-NRG1</i>		None	1b	–	+
5	AD13-223T	F	53	Never	<i>CD74-NRG1</i>		None	1a	–	+
6	AD13-379T	F	66	Never	<i>SLC3A2-NRG1</i>	t(8;11)(p12;q13)	None	1b	Not tested	Not tested
7	436T	M	61	Ever (41)	<i>EZR-ERBB4</i>	t(2;6)(q25;q34)	None	1b	–	+
8	AD08_127T	F	66	Never	<i>TRIM24-BRAF</i>	inv7(q33;q34)	None	1a	+	+
9	AD12-119T	M	62	Current (63)	<i>KIAA1468-RET</i>	t(10;18)(q21;q11)	None	1a	+	–

^aEGFR, KRAS, BRAF, and HER2 mutations and ALK, RET, and ROS1 fusions.

NRG1 fusion-positive cases were preferentially from female never smokers (Table 1).

The *CD74-NRG1* and *SLC3A2-NRG1* fusion proteins, whose sequences were deduced from RNA sequencing data, contained the *CD74* or *SLC3A2* transmembrane domain and retained the EGF-like domain of the *NRG1* protein (*NRG1* III- β 3 form; Fig. 1A). The *NRG1* III- β 3 protein has a cytosolic N-terminus and a membrane-tethered EGF-like domain, and mediates juxtacrine signals signaling through *HER2:HER3* receptors (19). Because parts of *CD74* or *SLC3A2* replaced the transmembrane domain of wild-type *NRG1* III- β 3, we speculated that the membrane-tethered EGF-like domain might activate juxtacrine signaling through *HER2:HER3* receptors. In addition, it was also possible that expression of these fusion proteins resulted in the production of soluble *NRG1* protein due to proteolytic cleavage at sites derived from *NRG1* (dashed green lines in Fig. 1A), as recently suggested for *NRG1* type III proteins (20, 21). Exposing EFM-19 cells to conditioned media from H1299 human lung cancer cells expressing exogenous *CD74-NRG1* fusion protein resulted in phosphorylation of endogenous *ERBB2/HER2* and *ERBB3/HER3* proteins, suggesting that autocrine *HER2:HER3* sig-

naling was activated by secreted *NRG1* ligands generated from *CD74-NRG1* polypeptides (Fig. 2A). Phosphorylation of extracellular signal-regulated kinase (ERK) and AKT, downstream mediators of *HER2:HER3*, was also elevated. *HER2*, *HER3*, and ERK phosphorylation was suppressed by lapatinib and afatinib, U.S. Food and Drug Administration (FDA)-approved tyrosine kinase inhibitors (TKI) that target *HER* kinases (22–24). Together, these observations indicate that *NRG1* fusions activated *HER2:HER3* signaling by juxtacrine and/or autocrine mechanisms.

The *EZR-ERBB4* fusion protein contained the *EZR* coiled-coil domain, which functions in protein dimerization, and also retained the full *ERBB4* kinase domain (Fig. 1A). These features indicated that the *EZR-ERBB4* protein is likely to form a homodimer via the coiled-coil domain of *EZR*, causing aberrant activation of the kinase function of *ERBB4*, similar to the situation of *EZR-ROS1* fusion (5). Indeed, when the *EZR-ERBB4* cDNA was exogenously expressed in NIH3T3 fibroblasts, tyrosine 1258, located in the activation loop of the *ERBB4* kinase site, was phosphorylated in the absence of serum stimulation, indicating that fusion with *EZR* aberrantly activated the *ERBB4* kinase (Fig. 2B). Consistent with this, phosphorylation of a downstream

Table 2. Characteristics of 90 invasive mucinous LDACs

Variable	Mutation				Fusion					None (%)
	All	KRAS	BRAF	EGFR	<i>CD74-NRG1</i> or <i>EZR-SLC3A2-NRG1</i>	<i>TRIM24-ERBB4</i>	<i>BRAF</i>	<i>ALK</i>	<i>EML4-KIAA1468-RET</i>	
Total	90 (100)	56 (62.2)	2 (2.2)	1 (1.1)	6 (6.7)	1 (1.1)	1 (1.1)	1 (1.1)	1 (1.1)	21 (23.3)
Age (mean \pm SD; y)	67.2 \pm 9.7	68.1 \pm 9.7	66.5 \pm 3.5	50	61.2 \pm 11.5	61	66	64	62	68.1 \pm 9.6
Sex										
Male (%)	39 (43.3)	28 (50.0)	0 (0)	0 (0)	1 (16.7)	1 (100)	0 (0)	0 (0)	1 (100)	8 (38.1)
Female (%)	51 (56.7)	28 (50.0)	2 (100)	1 (100)	5 (83.3)	0 (0)	1 (100)	1 (100)	0 (0)	13 (61.9)
Smoking habit										
Never smoker (%)	51 (56.7)	29 (51.8)	2 (100)	1 (100)	4 (66.7)	0 (0)	1 (100)	1 (100)	0 (0)	13 (61.9)
Ever smoker (%)	39 (43.3)	27 (48.2)	0 (0)	0 (0)	2 (33.3)	1 (100)	0 (0)	0 (0)	1 (100)	8 (38.1)

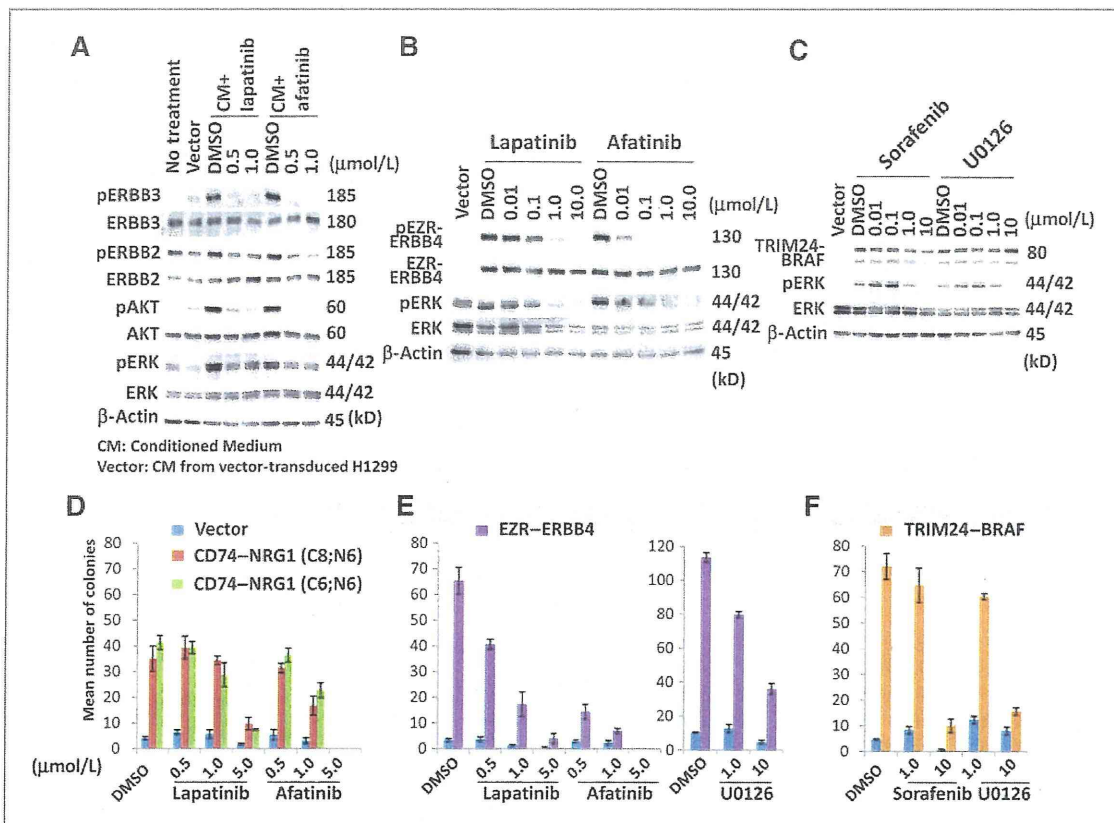


Figure 2. Oncogenic properties of gene-fusion products. A, ERBB3 activation by *CD74-NRG1* fusion, demonstrated using the EFM-19 cell system. ERBB3, ERBB2, AKT, and ERK phosphorylation were examined in EFM-19 (reporter) cells treated for 30 minutes with conditioned media from H1299 cells exogenously expressing *CD74-NRG1* cDNA. Phosphorylation was suppressed by HER-TKIs. B, ERBB4 activation by *EZR-ERBB4* fusion. Stably transduced NIH3T3 cells were serum-starved for 24 hours and treated for 2 hours with DMSO (vehicle control) or TKIs. Phosphorylation of ERBB4 and ERK was suppressed by ERBB4-TKIs. *EZR-ERBB4* protein was detected using an antibody recognizing ERBB4 polypeptides retained in the fusion protein. C, BRAF activation by *TRIM24-BRAF* fusion. Stably transduced NIH3T3 cells were serum-starved for 24 hours and treated for 2 hours with DMSO or kinase inhibitors. ERK phosphorylation (activation) was suppressed by sorafenib, a kinase inhibitor targeting BRAF, as well as by U0126, a MEK inhibitor. *TRIM24-BRAF* protein was detected using an antibody recognizing BRAF polypeptides retained in the fusion protein. D–F, anchorage-independent growth of NIH3T3 cells expressing *CD74-NRG1* (D), *EZR-ERBB4* (E), or *TRIM24-BRAF* (F) cDNA, and suppression of this growth by kinase inhibitors. Mock-, *CD74-NRG1*-, *EZR-ERBB4*-, and *TRIM24-BRAF*-transduced NIH3T3 cells were seeded in soft agar with DMSO alone or kinase inhibitors. Colonies > 100 μm in diameter were counted after 14 days. Column graphs show mean numbers of colonies \pm SEM.

mediator ERK was also elevated. Phosphorylation of ERBB4 and ERK was suppressed by lapatinib and afatinib, which inhibit ERBB4 protein (22–24).

The *TRIM24-BRAF* fusion protein retained the BRAF kinase domain but lacked the N-terminal RAS-binding domain responsible for negatively regulating BRAF kinase. These features suggested that the fusion was constitutively active, as in the cases of the *ESRP1-BRAF* and *AGTRAP-BRAF* fusions in other cancers (25). When the *TRIM24-BRAF* cDNA was exogenously expressed in NIH3T3 cells, ERK, a downstream mediator of BRAF, was phosphorylated in the absence of serum stimulation, indicating that fusion with *TRIM24* aberrantly activated BRAF kinase (Fig. 2C). ERK phosphorylation was suppressed by sorafenib, an FDA-approved drug originally

identified as a RAF kinase inhibitor (26), and also by the MEK inhibitor U0126 (Fig. 2C).

Exogenous expression of fusion gene cDNAs induced anchorage-independent growth of NIH3T3 fibroblasts, indicating their transforming activities (Fig. 2D–F). This growth was suppressed by the kinase inhibitors that suppressed fusion-induced activation of signal transduction, as described above. NIH3T3 cells expressing *EZR-ERBB4* or *TRIM24-BRAF* fusion cDNA formed tumors in nude mice (Fig. 3). Therefore, we concluded that these three fusions function as driver mutations in IMA development. We screened 200 commonly used human lung cancer cell lines, but all were negative for these three fusions (data not shown); thus, the oncogenic properties of these fusions remain unvalidated in human cancer cells.

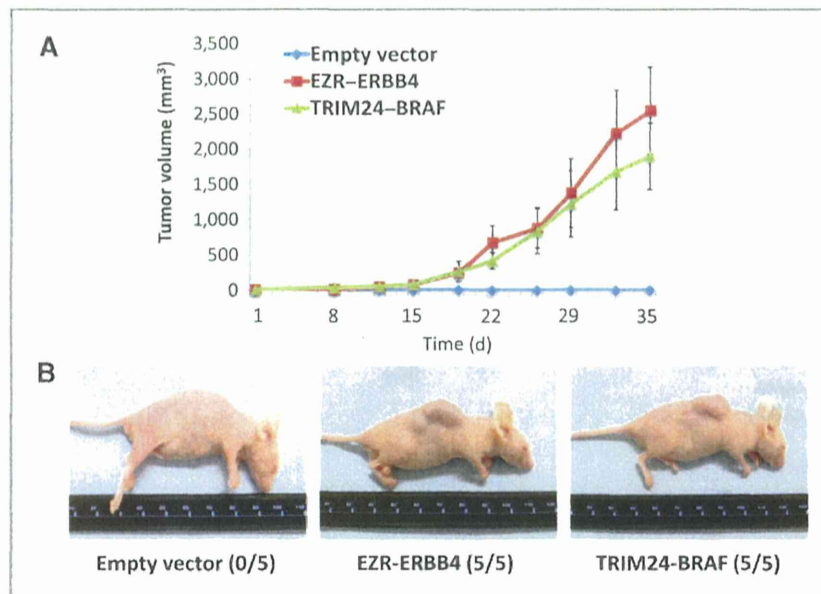


Figure 3. Tumorigenicity of NIH3T3 cells expressing *ERZ-ERBB4* or *TRIM24-BRAF* fusion cDNAs. **A**, tumor growth in nude mice injected with NIH3T3 cells expressing empty vector, *EZR-ERBB4* fusion, or *TRIM24-BRAF* fusion. Cells were resuspended with 50% Matrigel and injected into the right flank of nude mice. Tumor size was measured twice weekly for 5 weeks. Data are shown as mean \pm SEM. **B**, representative tumors were photographed on day 21. The numbers in parentheses indicate the ratio of the number of mice with tumors to the number of mice receiving cell injection.

The results here suggest that the *NRG1*, *ERBB4* and *BRAF* fusions are novel driver mutations involved in the development of IMAs of the lungs (Fig. 1C) and potential targets for existing TKIs. The recurrent *NRG1* fusions were especially notable because *NRG1* was previously identified as a regulator of goblet-cell formation in primary cultures of human bronchial epithelial cells (27); therefore, activation of the *NRG1*-mediated signaling pathway (s) might play a part in IMA development by contributing to both cell transformation and acquisition of goblet-cell morphology. In addition to a small fraction of known druggable aberrations (an *ALK* fusion and an *EGFR* mutation), more than 10% (11/90; 12.2%) of IMAs harbored other druggable aberrations targeted by existing kinase inhibitors: these aberrations were represented by fusions involving *NRG1*, *ERBB4*, *BRAF*, or *RET*, or *BRAF* mutations (Table 2, Fig. 1C). To facilitate translation of these findings to the cancer clinic, it will be necessary to establish diagnostic methods, particularly using break-apart and fusion FISH methods, capable of detecting these aberrations. Such methods will also help identify additional fusions involving other partner genes and contribute to a greater understanding of the significance of gene fusions in lung carcinogenesis.

Disclosure of Potential Conflicts of Interest

No potential conflicts of interest were disclosed.

References

- Pao W, Hutchinson KE. Chipping away at the lung cancer genome. *Nat Med* 2012;18:349–51.
- Shaw AT, Engelman JA. *ALK* in lung cancer: past, present, and future. *J Clin Oncol* 2013;31:1105–11.
- Gautschi O, Zander T, Keller FA, Strobel K, Hirschmann A, Aebi S, et al. A patient with lung adenocarcinoma and *RET* fusion treated with vandetanib. *J Thorac Oncol* 2013;8:e43–4.

Authors' Contributions

Conception and design: K. Tsuta, J. Yokota, T. Yoshida, T. Kohno

Development of methodology: H. Ichikawa

Acquisition of data (provided animals, acquired and managed patients, provided facilities, etc.): T. Nakaoku, K. Tsuta, H. Ichikawa, H. Sakamoto, K. Furuta, Y. Shimada, S.-I. Watanabe, H. Nokihara, K. Yasuda, M. Hiramoto, T. Nammo, T. Ishigame, H. Okayama

Analysis and interpretation of data (e.g., statistical analysis, biostatistics, computational analysis): T. Nakaoku, K. Tsuta, M. Enari, A.J. Schetter, C.C. Harris

Writing, review, and/or revision of the manuscript: T. Nakaoku, K. Tsuta, H. Ogiwara, S.-I. Watanabe, H. Nokihara, K. Yasuda, M. Hiramoto, A.J. Schetter, C.C. Harris, Y.H. Kim, M. Mishima, T. Yoshida, T. Kohno

Administrative, technical, or material support (i.e., reporting or organizing data, constructing databases): K. Tsuta, K. Shiraishi, M. Enari, H. Ogiwara, S.-I. Watanabe, H. Okayama

Study supervision: K. Tsuta, J. Yokota

Acknowledgments

The authors thank Suenori Chiku and Hirohiko Totsuka for the analysis of sequencing data and Dai Suzuki, Kazuko Nagase, Sachiyo Mitani, Sumiko Ohnami, Yoko Odaka, and Misuzu Okuyama for technical assistance.

Grant Support

This work was supported, in part, by the Advanced Research for Medical Products Mining Program of the National Institute of Biomedical Innovation (NIBIO), Grants-in-Aid from the Ministry of Health, Labor, and Welfare for the Third-term Comprehensive 10 year Strategy for Cancer Control and for Research for Promotion of Cancer Control Programs; and the Princess Takamatsu Cancer Research Fund.

The costs of publication of this article were defrayed in part by the payment of page charges. This article must therefore be hereby marked *advertisement* in accordance with 18 U.S.C. Section 1734 solely to indicate this fact.

Received January 14, 2014; revised March 22, 2014; accepted April 1, 2014; published OnlineFirst April 14, 2014.